

ISTITUTO NAZIONALE DI FISICA NUCLEARE

Sezione di Genova

INFN/FM-98/01
12 Maggio 1998

XPS AND AES ANALYSIS OF OZONIZED ULTRAPURE WATER TREATMENT OF NB SURFACE FOR SCRF CAVITIES

A. Daccà, G. Gemme, R. Parodi, K. Asano

**XPS AND AES ANALYSIS OF OZONIZED ULTRAPURE WATER TREATMENT
OF NB SURFACE FOR SCRF CAVITIES**

A. Daccà, G. Gemme, R. Parodi

INFN - Sezione di Genova, via Dodecaneso 33, I-16146 Genova (Italy)

K. Asano

KEK, National Laboratory for High Energy Physics

Oho, 1 - 1, Tsukuba-shi, Ibaraki-ken, 305, Japan

A B S T R A C T

The main elements in surface contamination of Nb superconducting cavities are oxygen and carbon; recently a new surface treatment has been proposed for KEK B-factory (KEKB - Japan) to reduce carbon contamination, that is responsible of electron emission and photon stimulated desorption (PSD) yield. This treatment consists of rinsing the cavities after the electropolishing with ozonized ultrapure water (OUR); the AES (Auger Electron Spectroscopy) measurements performed at KEK show a strong reduction of carbon contamination and a passivation effect of the Nb₂O₅ layer grown on the Nb surface.

The XPS - AES system of the INFN - Sezione di Genova is a useful tool to check the results obtained at KEK; in particular the XPS technique allows to identify the chemical states of the surface elements and, therefore, it is possible to collect more information about the Nb surface state. The work described in this Internal Note concerns the XPS - AES measurements performed on two different Nb samples (one rinsed with ultrapure water after the EP and the other rinsed with ozonized ultrapure water after the EP), about one month after the preparation (during this time they have been kept in a teflon tube filled with dry nitrogen).

1 . - INTRODUCTION

The surface treatments of Nb for superconducting RF cavities greatly influence the performance; the requirements to obtain high fields (for example, higher than about 10MV/m for 508MHz cryomodules at 4.2K) and to reduce RF losses are very pure niobium with very low surface contamination. Therefore it is important to study the consequences of the preparation methods of RF cavities and to know the chemical composition and the physical structure of Nb surface after common surface treatments. XPS (X-ray Photoelectron Spectroscopy) and AES (Auger Electron Spectroscopy) allow to investigate the chemical composition of a surface (the penetration depth of these techniques is of the order of 15 - 20 monolayers) in a non destructive way and give information both on the elements present on the surface and on their chemical state ⁽¹⁾. The use of ARXPS (Angle Resolved X-ray Photoelectron Spectroscopy), moreover, permits to analyse the in-depth composition and to calculate the thickness of different layers detected on the surface.

The usual surface treatments for Nb RF cavities are the chemical polishing (CP), the electropolishing (EP), the oxipolishing (OP) and anodic oxidation followed by rinsing with ultrapure water ⁽²⁾. The Nb surface state after these treatments has already been carefully investigated in precedent works ⁽³⁾.

Recently a new surface treatment for superconducting cavities has been proposed at KEK ⁽⁴⁾; this treatment consists in using ozonized ultrapure water (OUR) for rinsing the cavities after EP, instead of rinsing in a H₂O₂ solution. It has been found ⁽⁵⁾ by AES analyses that this method removes completely the carbon contamination and produces a clean, stable, dense, thin ($\approx 40\text{\AA}$) and amorphous Nb₂O₅ layer on the electropolished Nb surfaces. In this way it is possible to reduce the photon stimulated desorption (PSD) yield and the field emission from Nb surfaces. Finally the OUR treated cavities exposed to air up to 4 days at 1 atm did not show degradation in the performance.

In the present work we show the results of XPS and AES measurements performed on two different Nb samples: the first (indicated with EP) was rinsed in ultrapure water after EP, the second (indicated with OUR) was rinsed in ozonized ultrapure water (2.9ppm O₃, 15 min. for these samples) after the EP. Both the samples were kept in a teflon tube filled with dry nitrogen for more than one month. The aim of the present study is to detect differences between the two methods of rinsing, to verify the results obtained with the AES technique at KEK and,

eventually, to show that the OUR treatment passivate the Nb surface also for long periods of time.

The samples, which are kept in an UHV sample chamber for the transport and treated with OUR for longer rinsing time and higher ozone concentrations, will be also measured to investigate the surface carbon contamination.

2. - RESULTS AND DISCUSSION

2.1. - XPS measurements

XPS and AES analyses on Nb samples were performed on a PHI 5600ci ESCA spectrometer; the careful description of the XPS experimental set-up has been reported previously ⁽⁶⁾. The AES system consists of an electron gun that produces an electron beam by thermoionic emission from a LaB₆ filament. The accelerating voltage applied to the beam can vary between 1 and 10 kV, while the Auger electrons emitted from the surface are collected by the SCA (Spherical Capacitor Analyser) electron energy analyser. A SED (Secondary Electron Detector) is mounted on the spectrometer and allows to take SEM (Scanning Electron Microscopy) images. The base pressure inside the analysis chamber is 2×10^{-10} Torr.

The samples EP and OUR were introduced in the spectrometer on the same sample holder and we performed the same measurements on them.

The first sample analyzed was that signed with EP: a first "Survey" spectrum was acquired (Fig. 2.1), that allows to identify the elements present on the surface. The more intense signals are produced by Nb, O and C, but also F, Na, S, Cu and Zn are detected on the surface. The atomic concentrations calculated from the spectrum of Fig. 1 as the area under the peaks, after a Shirley background subtraction ⁽⁷⁾, are reported in Table 2.1. The values in parenthesis are the sensitivity factors of the spectrometer, while the values below them are the concentrations expressed as at.%. The concentrations of the "impurities" (the elements different from Nb, O and C) are of the order of 0.5 - 2 at.%.

After this preliminary acquisition, we performed an XPS analysis on the principal lines of the identified elements: Nb3d, O1s, C1s, Cu2p, Na1s, F1s, S2p, Zn2p_{3/2} in order to improve the signal/noise ratio. In this way we are able to perform a deconvolution of these lines and reveal the different chemical states that contribute to the XPS signal. The deconvolution on the Nb3d

line (Fig. 2.2) reveals that there are three chemical states that contribute to the Nb signal: the Nb line ($E_B = 201.9\text{eV}$) represented by bands 1 and 2, the NbO line ($E_B = 203.2\text{eV}$) represented by bands 3 and 4 and the Nb₂O₅ line ($E_B = 207.4\text{eV}$) represented by bands 5 and 6. The parameters of these bands are reported in Table 2.2.

NB_EP1~1.SPE: Sample ultrapure water rinsed							INFN Genova
98 Mar 20	Al mono	350.0 W	0.0 μ	45.0°	117.40 eV	9.5812e+004 max	18.07 min
Sur1/Full/1							

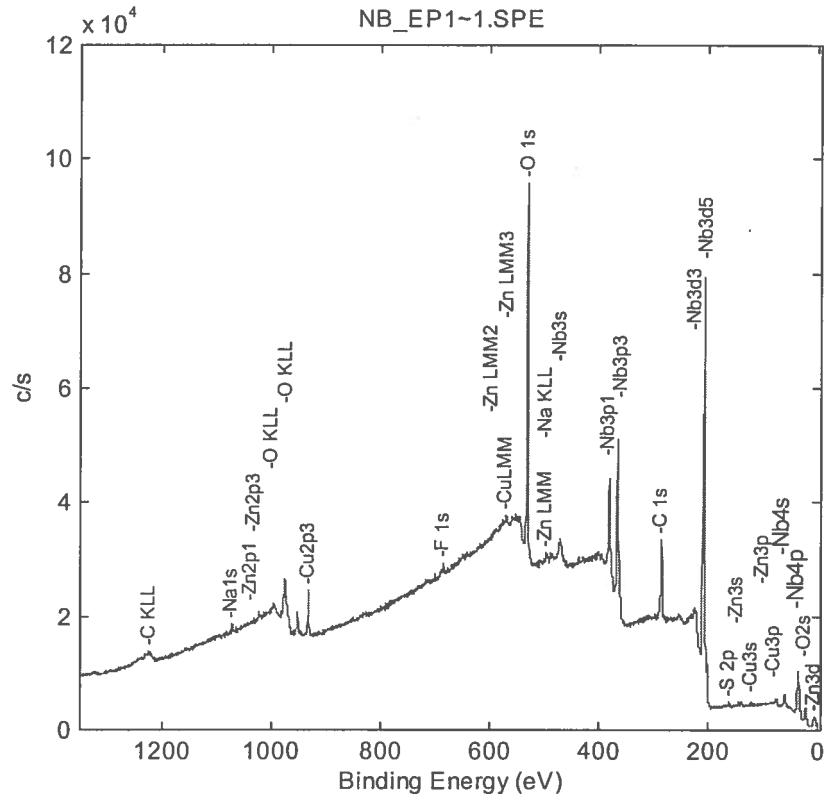


Figure 2.1. XPS survey of the sample rinsed with ultrapure water after EP.

Atomic concentration Table							
C1s	O1s	F1s	Na1s	S2p	Cu2p3	Zn2p3	Nb3d
[0.314]	[0.733]	[1.000]	[1.102]	[0.717]	[2.626]	[2.768]	[3.127]
27.75	47.37	1.63	0.60	1.47	1.69	0.25	19.24

Table 2.1. Atomic concentrations of the elements detected on the EP sample.

The deconvolution of the O1s line is reported in Fig. 2.3: there are three different chemical states that contribute to the line-shape of the O signal. They are the Nb₂O₅ line ($E_B = 530.6\text{eV}$, band 1), the OH line ($E_B = 532.9\text{eV}$, band 3) and the line at $E_B = 531.6\text{eV}$ (band 2) that is probably produced by Na₂SO₄ ($E_B = 531.4\text{eV}$), but it could also be the Na₂CO₃ signal ($E_B = 531.6\text{eV}$). The parameters of these lines are in Table 2.3.

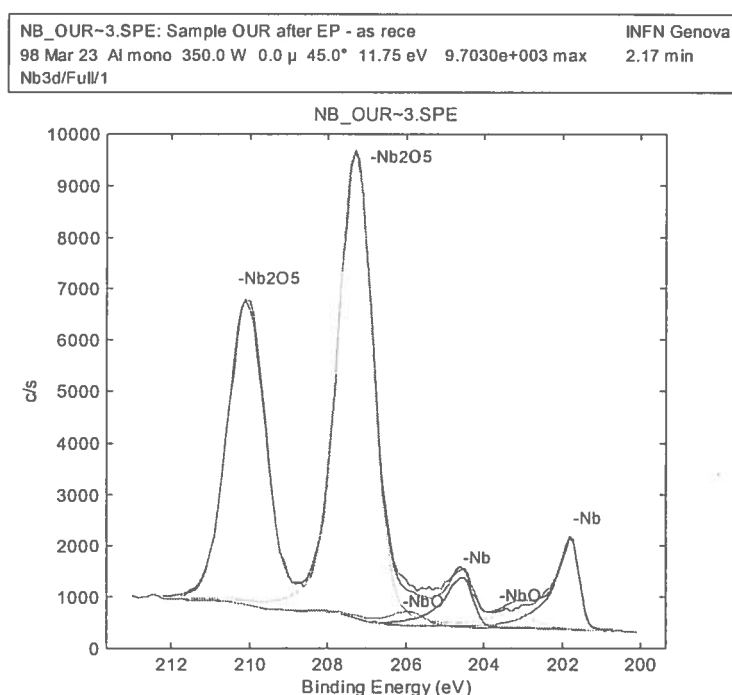


Figure 2.2. Deconvolution of the Nb3d line.

Curve Fit Summary										
Band	Pos	Delta	B_FWHM	G_FWHM	Height	Area	%Gauss	TLength	TScale	%Area
1	201.75	0.00	0.63	0.44	1743	1496	92	20.00	0.8552	7.14
3	203.17	1.42	1.17	0.92	328	581	45	22.14	0.5000	2.77
2	204.50	2.75	0.81	0.52	944	988	80	16.12	1.1000	4.71
4	205.92	4.17	1.09	0.92	271	383	100	18.90	0.4987	1.83
5	207.28	5.53	1.02	0.99	8776	10544	80	10.00	0.1377	50.33
6	210.03	8.28	1.10	1.01	5697	6959	90	4.60	1.1000	33.21

Table 2.2. Curve fit parameters of the Nb bands reported in Fig. 2.2.

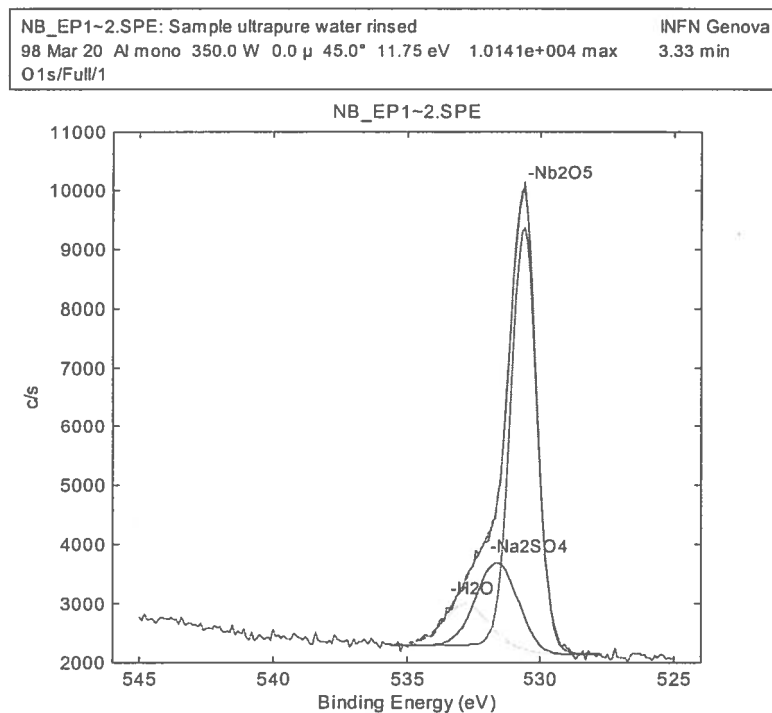


Figure 2.3. Deconvolution of the O1s line.

Curve Fit Summary									
Band	Pos	Delta B	FWHM G	FWHM	Height	Area	%Gauss	%Area	ChiSquared
1	530.61	0.00	1.05	1.05	7228	8941	78	68.78	2.636
2	531.60	0.99	1.78	1.78	1659	3170	98	24.38	
3	532.96	2.35	1.45	1.45	569	889	98	6.84	

Table 2.3. Curve fit parameters of the O bands reported in Fig. 2.3.

Finally we operated the deconvolution of the C1s line (Fig. 2.4). This line is the superposition of three different chemical states: the principal contribution is given by the graphite signal ($E_B = 285.0\text{eV}$, band 1), while the other two lines are probably produced by C - H bonds ($E_B = 286.5\text{eV}$, band 2) and by C - F bonds or carbonates such as Na_2CO_3 ($E_B = 288.8\text{eV}$, band 3). The summary of the deconvolution of the C1s line is reported in Table 2.4.

NB_EP1~2.SPE: Sample ultrapure water rinsed
 98 Mar 20 Al mono 350.0 W 0.0 μ 45.0° 11.75 eV 3.1493e+003 max 4.67 min
 C1s/Full/1

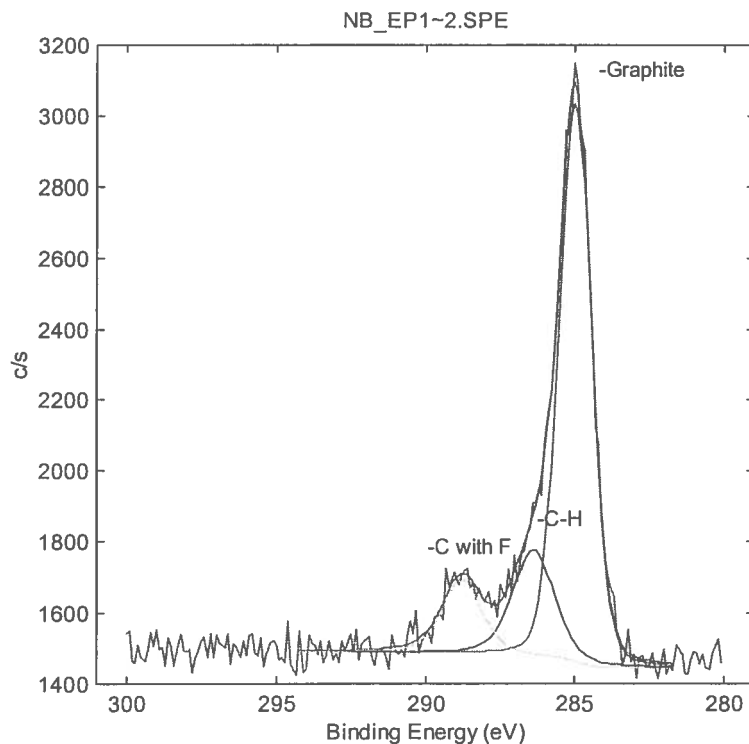


Figure 2.4. Deconvolution of the C1s line.

Curve Fit Summary									
Band	Pos	Delta B	FWHM	G_FWHM	Height	Area	%Gauss	%Area	ChiSquared
1	285.01	0.00	1.29	1.29	1598	2423	79	73.27	1.005
2	286.49	1.49	1.44	1.44	284	521	59	15.77	
3	288.82	3.81	1.44	1.44	205	363	68	10.96	

Table 2.4. Curve fit parameters of the C bands reported in Fig. 2.4.

The Zn2p_{3/2} line and the F1s line are reported in Figs. 2.5 - 2.6. These elements show only one chemical state that corresponds to the compound ZnF₂, both for the Zn line ($E_B = 1022.8\text{eV}$) and for the F line ($E_B = 685.1\text{eV}$).

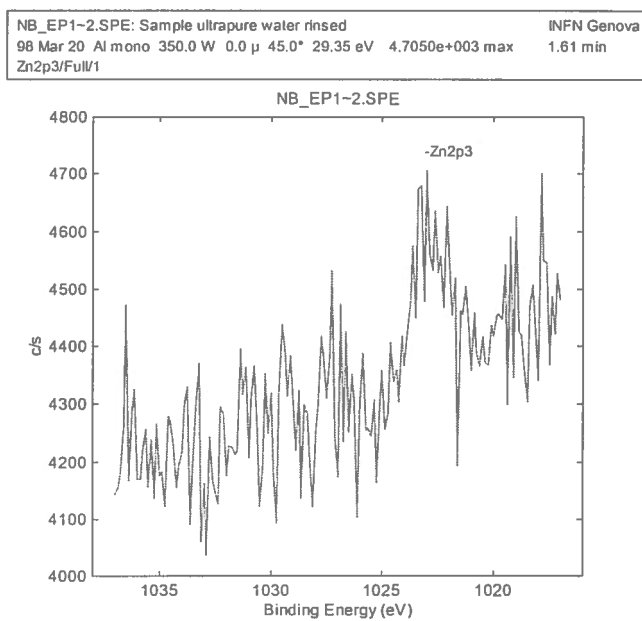


Figure 2.5. The Zn2p3 line of the sample rinsed with ultrapure water after EP.

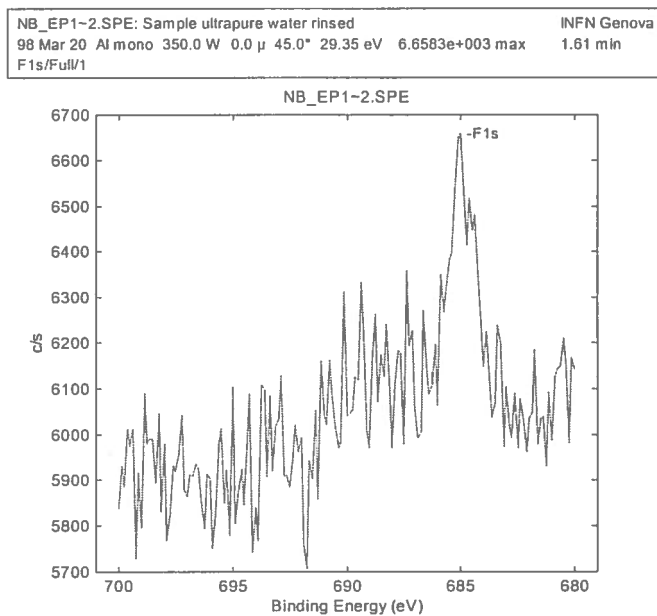


Figure 2.6. The F1s line of the sample rinsed with ultrapure water after EP.

The position of the Na1s line (Fig. 2.7) could be consistent with the compounds Na_2S or Na_2CO_3 .

Finally we operated the deconvolution of the S2p line (Fig. 2.8) that shows two different chemical states, one typical of the sulfides (Na_2S , $E_B = 161.8\text{eV}$) and the other typical of the sulfates (Na_2SO_4 , $E_B = 168.8\text{eV}$). The parameters relative to the deconvolution of the S2p line are reported in the Table 2.5.

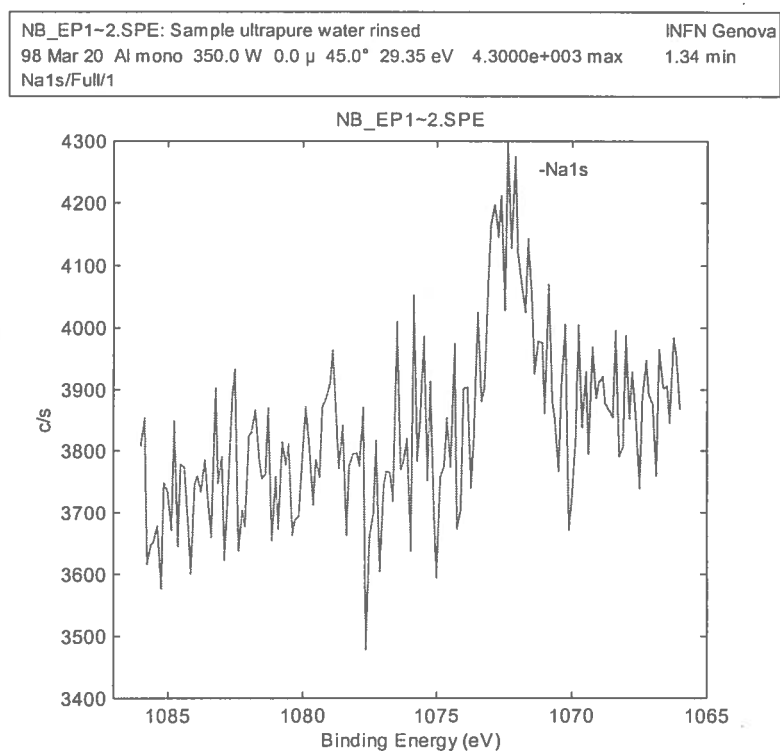


Figure 2.7. The Na1s line of the sample rinsed with ultrapure water after EP.

Curve Fit Summary									
Band	Pos	Delta	B_FWHM	G_FWHM	Height	Area	%Gauss	%Area	ChiSquared
1	161.81	0.00	1.65	1.65	182	401	48	39.58	0.926
2	162.99	1.18	1.72	1.72	88	200	48	19.79	
3	168.58	6.78	1.79	1.79	115	274	48	27.08	
4	169.76	7.96	1.46	1.46	71	137	48	13.54	

Table 2.5. Curve fit parameters of the S bands reported in Fig. 2.8.

NB_EP1~2.SPE: Sample ultrapure water rinsed		INFN Genova
98 Mar 20	Al mono 350.0 W 0.0 μ 45.0° 29.35 eV 1.1762e+003 max	2.15 min
S2p/Full/1		

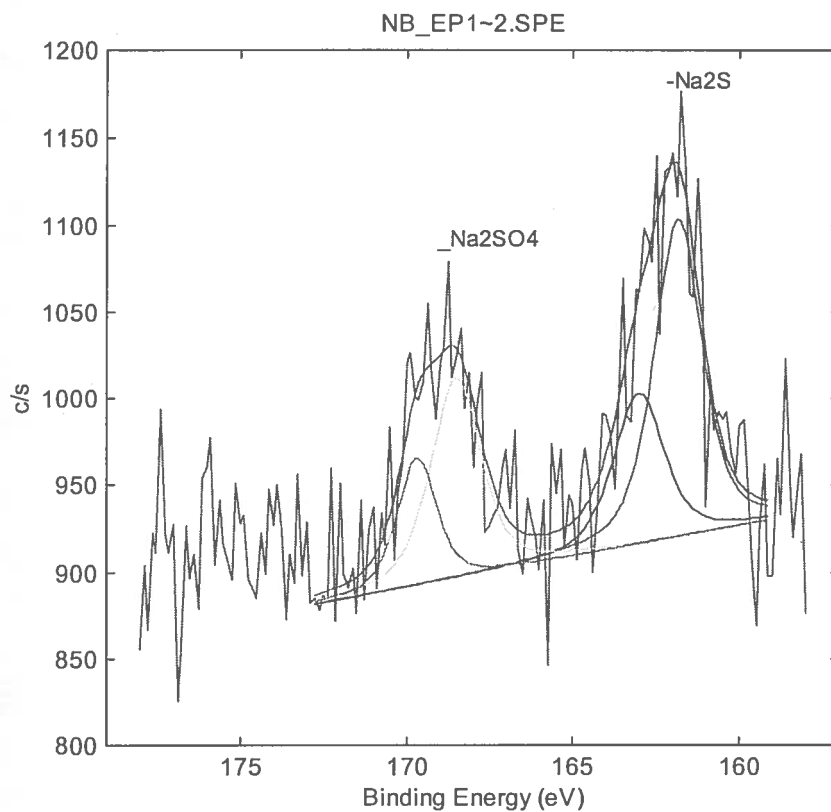


Figure 2.8. Deconvolution of the S2p line.

After these analyses we performed an angle-resolved analysis to quantify the thickness of the compound present on the EP sample.

The atomic concentrations of the elements revealed with the precedent analyses vs. the take-off angle (the angle between the sample surface and the axis of the analyser) are reported in Table 2.6 and in Fig. 2.9. From the table it is evident that the concentrations of the impurities (Cu, Na, S, F, and Zn) decrease with increasing the take-off angle and this proves that these elements are positioned in the first monolayers of the sample.

Take-off angle	Nb3d (at%)	C1s (at%)	O1s (at%)	Cu2p (at%)	Na1s (at%)	F1s (at%)	S2p (at%)	Zn2p3 (at%)
25	15.4922	40.4414	38.5442	2.2983	0.4217	0.7532	1.7715	0.2776
35	19.6298	32.2974	44.1665	1.5606	0.3559	0.2601	1.7297	0
45	21.3097	28.0832	47.0974	1.6003	0.4599	0.2342	1.1202	0.0951
55	23.6576	25.2794	47.6383	1.13	0.5156	0.6622	0.9357	0.1812
65	24.7894	22.2557	49.8138	1.4194	0.5785	0.4588	0.5158	0.1686
75	24.9339	21.936	50.429	0.9429	0.6425	0.2776	0.668	0.1701

Table 2.6. Atomic concentrations calculated for the different take-off angles for the EP sample.

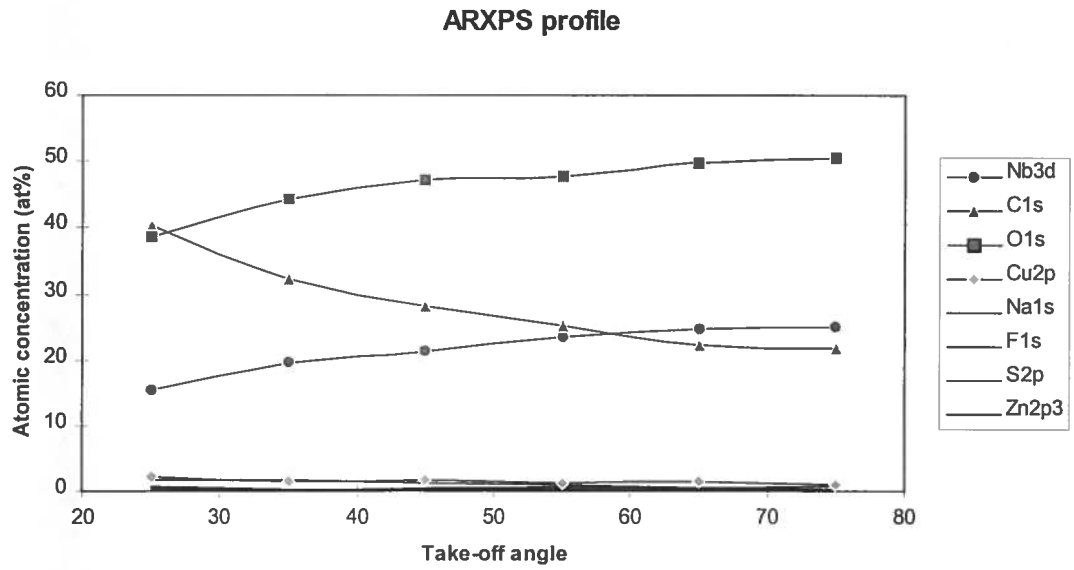


Figure 2.9. ARXPS profile of the EP sample.

By means of the equation ^[8]:

$$\frac{d_A}{\lambda_A \sin \theta} = \ln \left(1 + \frac{X_A}{X_B} \right) \quad (1)$$

we obtain the thickness (d_A) of an overlayer A on a substrate B, knowing the attenuation length λ_A of the photoelectrons coming from the overlayer (in this case we do not take into account the difference in the attenuation length of electrons coming from the substrate and traveling in the overlayer). In eq. (1) θ is the take-off angle and X_A and X_B are the atomic concentration of the elements A and B at the angle θ .

In our case eq. (1) was used to determine the thickness of the carbon layer on the Nb oxidized surface, as Fig. 2.9 shows that the C atomic concentration diminishes with the take-off angle.

The thickness that we obtained for the C layer of the EP sample was 5 monolayers equivalent.

To calculate the thickness of the NbO layer, positioned on the Nb surface, and of the Nb₂O₅ layer, above the NbO, we operated the deconvolution of the Nb3d lines at the different take-off angles. The atomic concentrations vs. the angles are reported in Fig. 2.10.

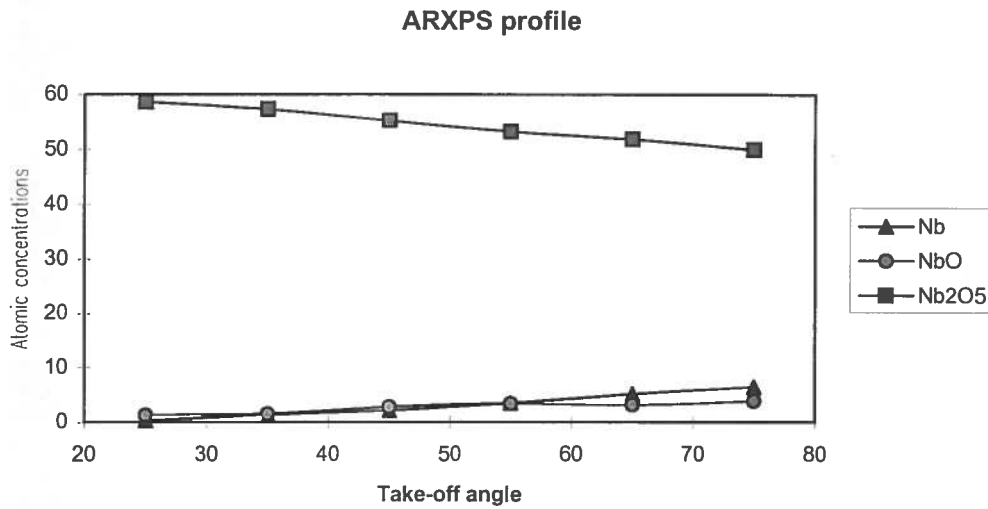


Figure 2.10. Atomic concentrations of the Nb chemical states vs. take-off angle for the EP sample.

In the case of a stack of oxides i (Nb oxides for our samples) on a substrate u (Nb) the thickness of the different layer can be expressed by the formula ^[9]:

$$\frac{d_i}{\lambda_i \sin \theta} = \ln \left[1 + \frac{X_i}{X_u} T_2 T_3 \cdots T_{i-1} \right] \quad (2)$$

where $T_i = \exp(-d_i/\lambda_i \sin \theta)$ is the transmission coefficient for the i^{th} layer.

Using eq. (2) and the atomic concentration of the Nb oxides measured with the ARXPS profile, we can evaluate that above the Nb surface of the EP sample there is a layer of NbO of the order of 3 monolayers equivalent and above this a layer of Nb₂O₅, about 13 monolayers thick. The layer of C (about 5 monolayers) is localized above the Nb oxides.

NB_OUR~2.SPE: Sample OUR after EP - as rece	INFN Genova
98 Mar 23 Al mono 350.0 W 0.0 μ 45.0° 117.40 eV 1.0108e+005 max	18.07 min
Sur1/Full/1	

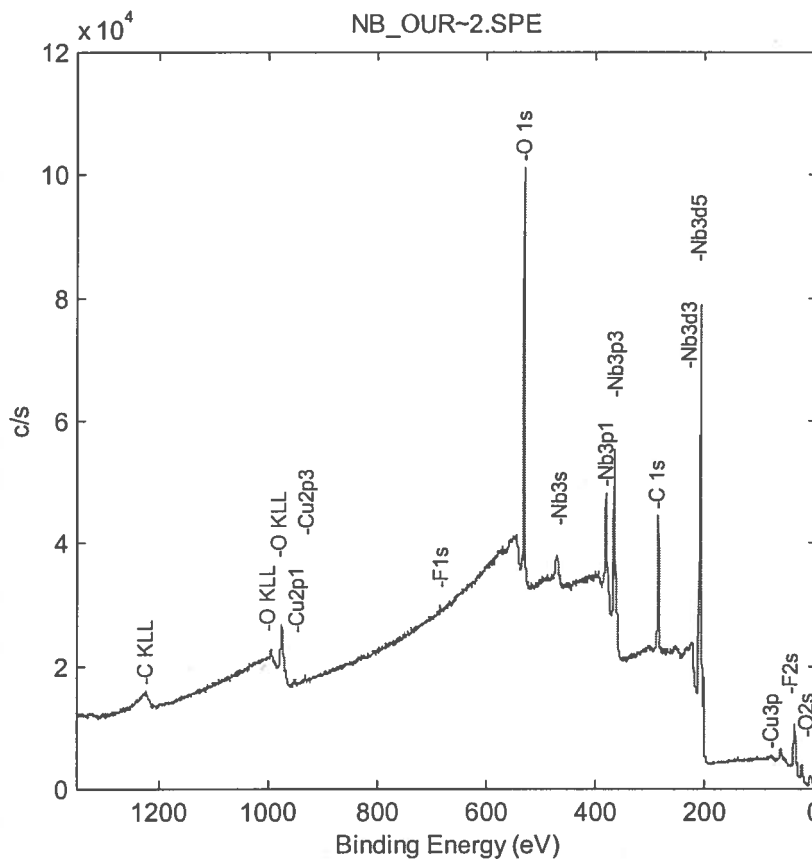


Figure 2.11. XPS survey of the OUR sample.

On the sample signed with OUR we performed the same measurements done on the EP sample. The Survey spectrum (Fig. 2.11) allows to identify the chemical elements present on the surface: Nb, O, C, and few traces of Cu and F. The atomic concentration of these elements, reported in Table 2.7, show that the contamination of this sample, in terms of impurities (Cu, Na, S, F, and Zn), is less than the EP sample, while the concentrations of O and C are of the same order for the two sample.

Atomic Concentration Table				
C1s	O1s	F1s	Cu2p	Nb3d
[0.314]	[0.733]	[1.000]	[4.395]	[3.127]
35.65	42.17	0.69	0.22	21.26

Table 2.7. Atomic concentrations of the elements detected on the OUR sample.

The deconvolution of the Nb3d line puts in evidence the existence of three chemical states: Nb, NbO, Nb₂O₅, the same identified for the EP sample and with similar parameters.

The deconvolution of the O1s line and the C1s line shows that the line-shape of this elements is similar to those of the EP sample and the parameters of the deconvolution are reported in Tables 2.8 and 2.9, respectively.

Curve Fit Summary									
Band	Pos	Delta	B_FWHM	G_FWHM	Height	Area	%Gauss	%Area	ChiSquared
1	530.59	0.00	1.13	1.13	7872	9913	89	77.92	1.707
2	531.69	1.11	1.59	1.59	1157	2003	95	15.75	
3	532.67	2.08	1.42	1.42	477	806	75	6.33	

Table 2.8. Curve fit parameters of the O bands detected on the OUR sample.

Curve Fit Summary									
Band	Pos	Delta	B_FWHM	G_FWHM	Height	Area	%Gauss	%Area	ChiSquared
1	285.01	0.00	1.14	1.14	2542	3282	86	82.70	1.030
2	286.30	1.29	1.46	1.46	267	454	80	11.45	
3	288.81	3.80	1.46	1.46	146	232	95	5.85	

Table 2.9. Curve fit parameters of the C bands detected on the OUR sample.

The angle-resolved profile, performed to quantify the thickness of the carbon and Nb oxides layers, is summarized in Fig. 2.12 and in Table 2.10.

The thickness of the carbon layer (above the Nb oxides), calculated by using eq. (1), is found to be 5 monolayer equivalent, as in the EP sample. The atomic concentrations deduced from the deconvolution of the Nb3d line are reported in Fig. 2.13. From these concentrations the

thickness of the NbO layer (eq. (2)) is about 3-4 monolayer equivalent and above this there is a layer of Nb₂O₅, whose thickness is of the order of 7 monolayers equivalent.

Take-off angle	Nb3d (at%)	C1s (at%)	O1s (at%)
25	17.135	47.1807	35.6843
35	20.1472	38.853	40.9998
45	22.5983	33.2027	44.199
55	24.1916	27.4439	48.3645
65	25.5527	25.5241	48.9232
75	24.545	26.017	49.438

Table 2.10. Atomic concentrations calculated for the different take-off angles for the OUR sample.

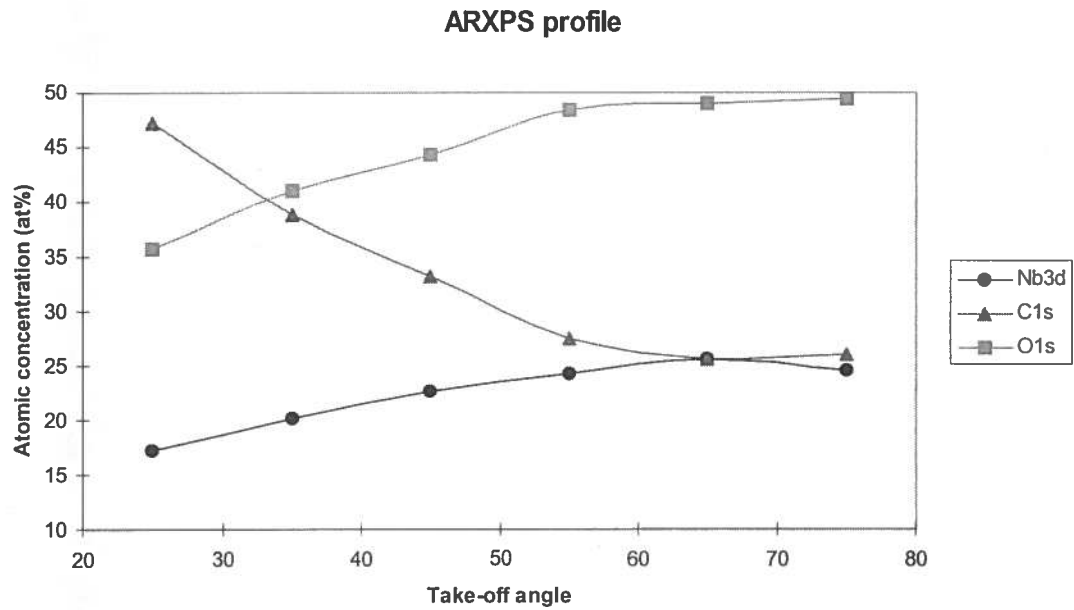


Figure 2.12. ARXPS profile for the OUR sample.

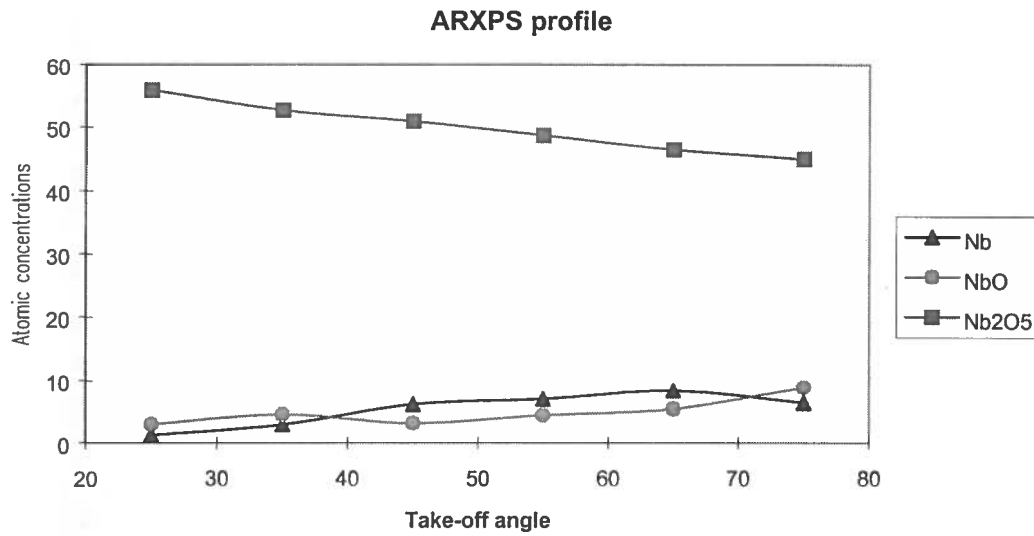


Figure 2.13. Atomic concentration of the Nb chemical states vs. the take-off angle for the OUR sample.

Therefore after this first group of analyses, that are non destructive, we can conclude that the main differences between the EP sample and the OUR sample are the following:

- a) the EP sample shows a higher contamination than the OUR sample in terms of impurities (Cu, Na, S, F, and Zn) different from carbon and oxygen;
- b) the line-shape of the principal lines of Nb, C and O is very similar for the two samples and the deconvolution of these lines is obtained with the same chemical states;
- c) the carbon layer is positioned above the Nb oxides and its thickness is the same for the two samples, that is about 5 monolayers equivalent;
- d) the NbO layer is positioned above the pure Nb surface and its thickness is of the order of 3 - 4 monolayers equivalent for the two samples;
- e) the Nb₂O₅ layer is positioned above the NbO layer and its thickness is very different for the two samples: it is 13 monolayers equivalent for the EP sample, while it decreases to about 7 monolayers equivalent in the OUR sample.

The ARXPS analysis seems to indicate that the carbon contamination is quantitatively the same on the two samples, 30 - 40 days after the surface treatments (during which they have been exposed mainly to air). Viceversa, as far as the oxygen contamination is concerned, we observe a great difference between the quantity of oxides, in particular Nb pentoxide, grown on the Nb surface during the period between the preparation and the analysis: there is a factor two between the thickness of the Nb₂O₅ layer on the EP sample and that on the OUR sample.

Finally we want to stress that we obtained the same results calculating the thickness' by means of a minimization procedure that takes into account the different attenuation lengths of the electrons in the substrate and in the overlayer (this procedure has been developed by J. Halbritter using the formula of Seah and Dench for the attenuations lengths ^[10]).

2.2. - AES measurements

In order to obtain more information on the sample composition and, moreover, to confirm the chemical composition calculated by means of the ESCA technique, the two samples were subjected to a series of AES analyses.

The AES measurements were performed with an electron beam energy of 9 KeV on a spot of 50 x 50 μm^2 ; this area was chosen to have the same dimensions of the area of acquisition of the ESCA technique (that is of the order of the X-ray monochromator spot, about 200 μm of diameter). In this way we can compare the results obtained with the two techniques.

The AES Survey spectrum acquired on the EP sample confirms the qualitative chemical analysis obtained with the XPS: the chemical elements identified on the surface, besides Nb, O and C, are F, Na, S, Cu, Zn and N (the last one not detected with the XPS).

The atomic concentrations deduced by the quantitative analysis of the AES spectrum are reported in Table 2.11 and reproduce approximately the composition of Table 2.1. The main difference consists in the atomic concentration of Nb, that is less if revealed by AES; this fact is quite reasonable, because the XPS sensitivity factor of Nb is 3.127, while the AES sensitivity factor is only 0.190. This means that the Auger technique has a better sensitivity for C and O, while the XPS one is more sensible to Nb.

Atomic Concentration Table								
C1	N1	O1	F1	Na1	S1	Cu1	Zn1	Nb1
[0.076]	[0.161]	[0.212]	[0.513]	[0.076]	[0.652]	[0.269]	[0.278]	[0.190]
36.06	0.74	50.74	0.31	2.57	1.14	2.36	0.70	5.38

Table 2.11. Atomic concentrations of the elements detected on the EP sample by AES analysis.

The same kind of measurement was performed on the OUR sample and the correspondent atomic concentrations are in Table 2.12.

Atomic Concentration Table				
C1	O1	F1	Cu1	Nb1
[0.076]	[0.212]	[0.513]	[0.269]	[0.190]
40.99	52.22	0.36	0.50	5.93

Table 2.12. Atomic concentrations of the elements detected on the OUR sample.

Also for the OUR sample it is evident that the AES analysis confirms the qualitative and quantitative chemical analysis performed with the XPS technique.

This means that the results obtained are consistent and reasonable.

2.3. - Sputtering profile

The XPS and AES techniques have a penetration depth of the order of 20 - 30 monolayers; by means of an ion gun (that is mounted on our spectrometer) it is possible to do an in - depth analysis, to know if the impurities detected on the EP sample are located in the first monolayers or if they are in the bulk of the sample.

We performed a sputtering profile with Ar^+ ions of 1.5 KeV and at the same time we acquired an XPS spectrum of the Nb3d, O1s and C1s lines.

The evolution of the atomic concentrations vs. the sputtering time is represented in Fig. 2.14.

We stopped the sputtering profile when we detected only a pure Nb signal; this was equivalent to about 30 minutes of sputtering time, with the parameters used for the ion gun (energy of the ions = 1.5 KeV, sputtering current = 0.35 μA).

After the sputtering we performed an XPS and an AES analyses; these spectra indicate that there are no more traces of impurities (F, Na, S, Cu and Zn) on the Nb surface, but only some percent of O and C, grown on the surface in the time between the end of the sputtering and the beginning on the acquisition, as reported in Table 2.13.

NB_EP1~1.PRO: Sputt 4x4 10mA 1KeV
 98 Apr 1 Al mono 350.0 W 0.0 μ 75.0° 29.35 eV 9.9770e+001 max

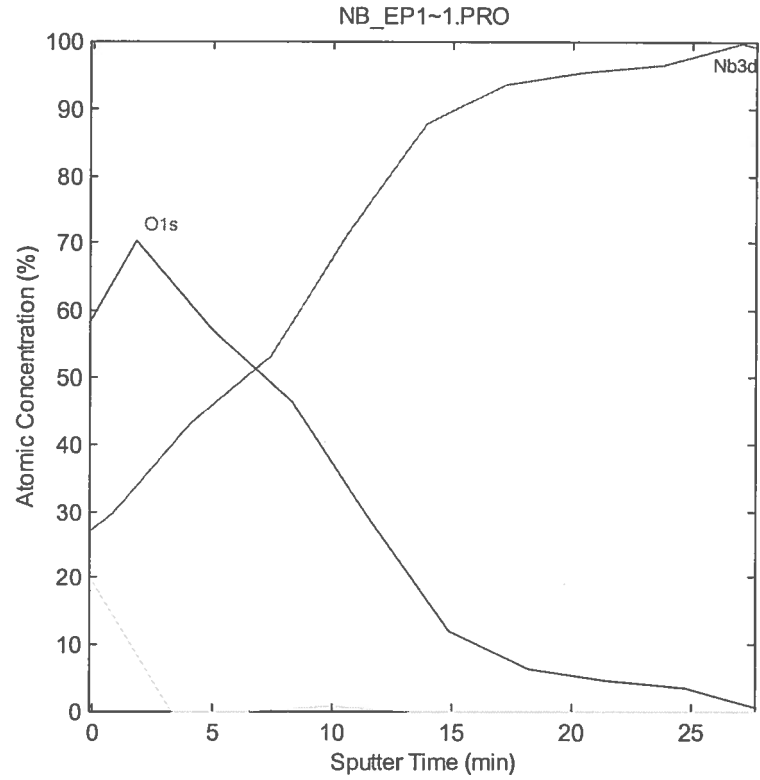


Figure 2.14. XPS sputtering profile on the EP sample.

Atomic Concentration Table							
C1s	O1s	F1s	Na1s	S2p	Cu2p	Zn2p3	Nb3d
[0.314]	[0.733]	[1.000]	[1.102]	[0.717]	[4.395]	[2.768]	[3.127]
1.85	2.82	0.00	0.00	0.06	0.25	0.00	95.04

Table 2.13. Atomic concentrations detected on the EP sample after a sputtering profile.

This result allows to conclude that the impurities detected on the EP sample were localized in the first monolayers and that, consequently, they were a residual product of the surface

treatments. A sputtering profile with the same parameters was performed on the OUR sample: the evolution of the atomic concentrations is similar to that reported in Fig. 2.14 and also in this case the sputtering time is of the order of 25 - 30 minutes.

3. - CONCLUSIONS

The XPS and AES analyses indicate that the EP sample contains a large number of impurities (F, Na, S, Cu and Zn) that are localized in the first atomic layers. The C contamination is mainly due to graphite and the C layer (5 monolayers thick) is positioned on the top of the Nb surface. Under this layer there are the Nb oxides: a layer of Nb pentoxide (13 monolayers thick) and under it a thin layer of Nb monoxide (3 - 4 monolayers). The OUR sample seems to be less contaminated: there are very few traces of impurities (F and Cu) and a minor amount of Nb oxides. The C layer on the top of the surface has the same thickness of the EP sample as the NbO layer just above the Nb surface; viceversa the Nb₂O₅ layer (positioned approximately between the NbO layer and the C layer) is only 7 monolayers thick.

The impurities found on the EP sample are a consequence of the surface treatments, while the high contamination by O and C, for both the samples, is probably due to the long period of exposure to air. A meaningful measurement, that allows to recognize the difference between different surface treatments performed on a Nb surface, has to be performed either immediately after the sample preparation or after a long period of time, if the sample is maintained in UHV and not exposed to air.

Therefore the present study shows that the OUR treatment surely reduces the surface contamination, but it cannot prevent the growth of C (mainly in form of graphite) on the Nb surface after a very long period of time (more than 30 days). In fact after one month the quantity of C on the OUR sample is the same that the one on the EP sample. Probably it is necessary to perform the OUR treatment for longer period of time and with higher ozone concentrations to obtain a stronger passivation of the surface (in order to keep the Nb at atmospheric pressure for period of one month or longer). The consequences of this kind of treatments are under study and will be published soon.

REFERENCES

- (¹) A. Daccà, G. Gemme, R. Parodi, Internal Note INFN/TC - 97/14, 7 May 1997.
- (²) P. Kneisel, Proc. Workshop on RF Superconductivity, KfK 3019, 27 (1980).
- (³) K. Asano, T. Furuya, Y. Kojima, S. Mitsunobu, H. Nakai, S. Noguchi, K. Saito, T. Tajima, M. Tosa, K. Yoshihara, KEK Report 88-2, (1988).
- (⁴) K. Asano, KEK Preprint, 93-216, March 1994 A.
- (⁵) K. Asano, E. Ezura, T. Furuya, H. Ishimaru, Y. Maeda, S. Mitsunobu, T. Tajima, T. Takahashi, KEK Preprint, 96-176, February 1997 A.
- (⁶) A. Daccà, G. Gemme, L. Mattera, R. Parodi, Internal Note, INFN/FM - 97/02, 7 May 1997.
- (⁷) D. A. Shirley, Phys. Rev. B, 5, 4709 (1972).
- (⁸) C. S. Fadley, Prog. Surf. Sci., 16, 3 (1984).
- (⁹) A. Darlinski, J. Halbritter, J. Vac. Sci. Technol. A, Vol. 5, No. 4 (1987), 1235.
- (¹⁰) M. P. Seah, W. A. Dench, Surf. Interface Anal., 1, 2 (1979).